HHS Public Access

Author manuscript

Circulation. Author manuscript; available in PMC 2017 January 05.

Published in final edited form as:

Circulation. 2016 January 5; 133(1): 82–97. doi:10.1161/CIRCULATIONAHA.115.016133.

The Estrogen Metabolite 16αOHE Exacerbates BMPR2-Associated PAH Through miR-29-Mediated Modulation of Cellular Metabolism

Xinping Chen, PhD[1], **Megha Talati, PhD**[1], **Joshua P. Fessel, MD, PhD**[1,2], **Anna R. Hemnes, MD**[1], **Santhi Gladson, MS**[1], **Jaketa French, BS**[1], **Sheila Shay, BS**[1], **Aaron Trammel, MDI**[3], **John A. Phillips, MD, PhD**[4], **Rizwan Hamid, MD, PhD**[4], **Joy D. Cogan, PhD**[4], **Elliott P. Dawson, MS**[5], **Kristie E. Womble, BS**[5], **Lora K. Hedges, BS**[4], **Elizabeth G. Martinez, DO**[6], **Lisa A. Wheeler, BS**[1], **James E. Loyd, MD**[1], **Susan J. Majka, PhD**[1], **James West, PhD**[1], and **Eric D. Austin, MD, MSCI**[4]

[1]Department of Medicine, Vanderbilt University Medical Center, Nashville, TN

[2]Department of Pharmacology, Vanderbilt University Medical Center, Nashville, TN

[3]Department of Medicine, Baylor College of Medicine, Houston, TX

[4]Department of Pediatrics, Vanderbilt University Medical Center, Nashville, TN

[5]Bioventures, Inc., Murfreesboro, TN

[6]Department of Pathology, Vanderbilt University Medical Center, Nashville, TN

Abstract

Background—Pulmonary arterial hypertension (PAH) is a proliferative disease of the pulmonary vasculature which preferentially affects females. Estrogens, such as the metabolite 16α-hydroxyestrone (16αOHE), may contribute to PAH pathogenesis; and, alterations in cellular energy metabolism associate with PAH. We hypothesized that 16αOHE promotes heritable PAH (HPAH) via miR-29 family upregulation, and that antagonism of miR-29 would attenuate pulmonary hypertension in transgenic mouse models of Bmpr2 mutation.

Methods and Results—MicroRNA (miR) array profiling of human lung tissue found elevation of miRs associated with energy metabolism, including the miR-29 family, among HPAH patients. miR-29 expression was 2-fold higher in Bmpr2 mutant mice lungs at baseline compared to controls, and 4 to 8-fold higher in Bmpr2 mice exposed to 16αOHE 1.25 μg/hr for 4 weeks. Blot analyses of Bmpr2 mouse lung protein showed significant reductions in PPARγ and CD36 in those mice exposed to 16αOHE, as well as from protein derived from HPAH lungs compared to

Correspondence: Eric D. Austin, MD, MSCI, Department of Pediatrics, Division of Pulmonary, Allergy, and Immunology Medicine, DD-2205 Medical Center North, Vanderbilt University School of Medicine, Nashville, TN 37232-2578, Phone: 615-343-7617, Fax: 615-343-9951, eric.austin@vanderbilt.edu.

Disclosures: EDA has grant funding from the NIH, Entelligence Award Program, and the American Thoracic Society. KEW and EPD hold two patents related to the isolation of miRNAs (Patent numbers: 8524448 and 8278035); Assignee: Bioventures, Inc.; Inventors: Elliott P. Dawson, Kristie E. Womble). XC, MT, JPF, SG, JF, SS, AT, JAP, RH, JDC, LKH, LAW, JEL, SJM, and JW report no relevant conflicts of interest.

controls. Bmpr2 mice treated with anti-miR-29 (α-miR29) (20mg/kg injections for 6 weeks) had improvements in hemodynamic profile, histology, and markers of dysregulated energy metabolism compared to controls. PASMCs derived from Bmpr2 murine lungs demonstrated mitochondrial abnormalities, which improved with α-miR29 transfection in vitro; endothelial-like cells derived from HPAH patient iPS cell lines were similar, and improved with α-miR29 treatment.

Conclusions—16αOHE promotes the development of HPAH via upregulation of miR-29, which alters molecular and functional indices of energy metabolism. Antagonism of miR-29 improves in vivo and in vitro features of HPAH, and reveals a possible novel therapeutic target.

Keywords

hypertension; pulmonary; estrogens; metabolism; microRNAs; models; animal

INTRODUCTION

Pulmonary arterial hypertension (PAH) is a progressive, devastating disease of the pulmonary vasculature that results in small vessel occlusion and loss, increasing pulmonary vascular resistance, and ultimately, death from right ventricular failure.[1] The two strongest risk factors for disease are mutations in the gene bone morphogenetic protein receptor type II (BMPR2) and female sex.[2, 3] BMPR2 mutations are the major association with the heritable form of PAH (HPAH). Among most PAH subtypes, the female to male ratio is skewed to favor females approximately 3:1.[4–6] Despite major advances in understanding the development of PAH, curative therapies remain elusive, and it is unclear why females are diagnosed more frequently. [7] The mechanisms of female predominance remain elusive, although an in depth understanding may provide a major therapeutic opportunity.[2]

We and others have shown that an abnormal sex hormone milieu contributes to PAH risk, and that modifying sex hormone exposures is a promising target.[8–15] Estrogen production and metabolism is a complex process that changes over time, and may occur in the sex-specific organs as well as peripherally[16]; for example, aromatase, the rate-limiting enzyme in the conversion of androgens to parent compound estrogens, is expressed in ovarian and extra-gonadal tissues including the lung.[8, 17] It was recently shown that variations in genes which contribute to estrogen signaling, associate PAH.[12, 13] Intriguingly, pulmonary artery smooth muscle cells from females with PAH express more aromatase compared to males, and aromatase inhibitor (anastrozole) treatment attenuates pulmonary hypertension (PH) in female rodent PH models.[8]

While parent compound estrogens appear important to PAH, so too may be certain estrogen metabolites. *BMPR2*-associated HPAH in females associated with reduced expression of the estrogen metabolism gene, CYP1B1[18], which may skew metabolism of parent estrogens into the estrogen metabolite 16α-hydroxyestrone (16αOHE). We demonstrated that preferential metabolism to 16αOHE associated with disease penetrance in HPAH.[12] In addition, chronic 16αOHE exposure significantly increased PH penetrance and severity in murine models of Bmpr2-associated PH.[19–22] 16αOHE's deleterious effects appear to involve both cellular processes and systemic abnormalities including suppression of cellular BMP signaling and alterations in energy metabolism, as well as induction of pulmonary vascular injury and

systemic insulin resistance.[22–24] Thus 16αOHE may promote cell-level alterations such as mitochondrial-metabolic abnormalities[25] which ultimately promote systemic metabolic abnormalities in PAH, including insulin resistance and hyperglycemia.[26–30]

The pathogenesis of PAH is likely a complex process involving the interplay of multiple factors including not only the circulating milieu but also environmental, genetic, and epigenetic factors which influence gene and protein expression. For example, there is emerging interest in the role of microRNA (miR) variation and activity in PAH. We sought to examine the relationship between 16αOHE-mediated estrogen signaling, altered energy metabolism, and PAH by first conducting unbiased miR expression arrays from the lung tissue of PAH patients and Bmpr2 mutant mice. We discovered a shared upregulation in both species of the miR-29 family which is known to regulate energy metabolism.[31, 32] We hypothesized that 16αOHE promotes HPAH via miR-29 family upregulation, and that antagonism of miR-29 would attenuate pulmonary hypertension in transgenic mouse models of Bmpr2 mutation.

METHODS

Human Study Population

Vanderbilt Pulmonary Hypertension Research Cohort study participants were recruited via the Vanderbilt Pulmonary Hypertension Center, while Vanderbilt Pulmonary Fibrosis Research Cohort study participants were recruited via the Vanderbilt Pulmonary Fibrosis Program. The VUMC Institutional Review Board approved all study protocols. All participants, or their surrogate custodians as appropriate, gave informed written consent to participate in genetic and clinical studies. Heritable PAH (HPAH) lung tissue samples (n = 2) were obtained following informed consent at the time of post-mortem autopsy. PAH was defined either by autopsy results showing plexogenic pulmonary arteriopathy in the absence of alternative causes such as congenital heart disease, or by clinical and cardiac catheterization criteria as previously published.[33] HPAH was considered the type of PAH if a subject met one or both of the following criteria: (a) family history of two or more subjects with confirmed PAH according to international standards of diagnostic criteria; or, (b) detection of a mutation in a PAH-specific gene, such as *BMPR2*. IPF lung tissue samples (n = 2) were obtained following informed consent at the time of lung transplantation. IPF was defined according to the joint guidelines of the American Thoracic Society and European Respiratory Society.[34] Both subjects had echocardiograms suggestive of normal right ventricular pressure, morphology, and function. Control lung tissue was isolated from donor lungs purchased commercially (n = 2) (Lonza, Allendale, NJ). The human lung donor subjects from all three groups were of female sex.

RNA extraction and preparation

Total RNA was isolated from 10 μm tissue sections using miRNeasy mini kit (Qiagen, Valencia, CA) according to manufacturer guidelines. In brief, sample incubation was performed in Xylene at 50°C to remove excess paraffin. Samples were washed in ethanol. Proteins were degraded by digestion buffer using protease solution as instructed. Isolation buffer and ethanol were used to bind samples to a spin-filter. DNAse treatment was used to

degrade DNA. The filter was washed several times and total RNA was eluted in 60 μL elution solution. Spectrophotometer was used to check total RNA quantity and quality (Nanodrop ND-1000; Thermo Scientific, Wilmington, DE). Prior to labeling and hybridization, samples were subject to RNA quality control in order to assess the integrity of the RNA, its content of small RNA and its concentration using Bioanalyzer (Agilent 2100 bioanalyzer) and NanoDrop™ instruments.

miRNA microarray assays

Exiqon Services was used for microRNA array profiling. All experiments were conducted at Exiqon Services, Denmark. The quality of the total RNA was verified by an Agilent 2100 Bioanalyzer profile. 250 ng total RNA from sample and reference was labeled with Hy3™ and Hy5™ fluorescent label, respectively, using the miRCURY LNA™ microRNA Hi-Power Labeling Kit, Hy3™/Hy5™ (Exiqon, Denmark) following the procedure described by the manufacturer. The Hy3™-labeled samples and a Hy5™-labeled reference RNA sample were mixed pair-wise and hybridized to the miRCURY LNA™ microRNA Array 6th Gen (Exiqon, Denmark), which contains capture probes targeting all microRNAs for human, mouse or rat registered in the miRBASE 16.0. The hybridization was performed according to the miRCURY LNA™ microRNA Array Instruction manual using a Tecan HS4800™ hybridization station (Tecan, Austria). After hybridization the microarray slides were scanned and stored in an ozone free environment (ozone level below 2.0 ppb) in order to prevent potential bleaching of the fluorescent dyes. The miRCURY LNA™ microRNA Array slides were scanned using the Agilent G2565BA Microarray Scanner System (Agilent Technologies, Inc., USA) and the image analysis was carried out using the ImaGene 9.0 software (BioDiscovery, Inc., USA). The quantified signals were background corrected (Normexp with offset value 10 [35]) and normalized using quantile normalization method, which we have found produces the best between-slide normalization to minimize the intensity-dependent differences between the samples. For murine tissue studies, Exiqon's miRCURY LNA™ microRNA Array (Exiqon, Vedbaek, Denmark) assays were performed after four weeks of gene activation in Rosa26-control and Rosa26-Bmpr2^{delx4+} mice. The mice had received four weeks of either vehicle (PEG) or 1.25 μg/hr 16αOHE. Each array consisted of a pool of 3 mice, and two arrays were used per condition.

Log-transformed miRNA expression data has previously been shown to be normally distributed, and so was treated as such for current statistical analyses[36]. miRNA probes with expression levels at the level of background were eliminated from array results provided by Exiqon. Using these results (196 probe sets for human data, 303 probe sets for mouse data), principal components analysis and creation of heat maps were done in JMP11 (SAS Institute).

Real-time reverse transcriptase-PCR (qRT–PCR)

Real time qRT–PCR was conducted on all samples to validate the miRNA profiling results. Specific miScript Primer Assays for miR-29a, miR-29b and miR-29c (Qiagen, Valencia, CA) were used to verify the expression by q-PCR. Reverse transcriptase (RT) reactions were performed with miScript II RT kit (Qiagen, Valencia, CA). The reactions were in 20 μl total volume containing 100 ng total RNAs (including small RNAs), 1X miScript HiSpec buffer

(1X miScript HiFlex buffer for RNU6B), 1X miScript Nucleics Mix, 1X miScript Reverse Transcriptase Mix. The reactions were incubated for 1 hour at 37°C, then 5 min at 95°C. All reverse transcriptase reactions were run in duplicate. Real-time PCR was performed on StepOnePlus Real-Time PCR System (Applied Biosystems). The PCR included the RT product, miScript SYBR Green and miScript Primer Assay (Qiagen, Valencia, CA). The reactions were incubated at 95°C for 10 min, followed by 40 cycles of 95°C for 15 s and 60°C for 1 min. Relative expression was determined using the ΔΔCT method. RNU6B was used as the internal control according to manufacturer instructions and consistent with prior studies.[37]

Western Blot Analyses

Mouse or human lung tissue were homogenized in RIPA buffer (PBS, 1% Ipegal, 0.5% sodium deoxycholate, 0.1% SDS) with proteinase and phosphatase inhibitor cocktails (Sigma-Aldrich St. Louis, MO). Protein concentration was determined by BCA protein assay (Thermo Scientific, Rockford, IL). Primary antibodies used for Western blot included: Glut4 (Abcam ab), CD36 (Novus NB400-144), Elastin (Abcam ab9514), PPARγ (Abcam ab27649), and β-Actin (Abcam ab8227).

Verification of miR-29 direct targets

The prediction of miRNA targets using bioinformatics algorithms has high false positive and false negative prediction rates.[38] Though false positive prediction can be excluded by experiments, false negative predictions would miss true targets. To further explore miR-29 potential direct targets, we employed a direct affinity purification method using a miRNA pull-down assay followed by specific quantitative PCR using established protocols.[39–41] In this approach, synthetic miRNA duplexes carrying a biotin group attached to the 3′ end of the miRNA sense strand were transfected into murine PVSMCs. This resulted in the sense strand's subsequent incorporation into the miRNA-induced silencing complex (miRISC). After cell lysis, the miRNA-mRNA complexes were captured on streptavidin beads from which the mRNA was purified and analyzed using quantitative RT-PCR analysis of the affinity purified mRNA. The genes PPARγ, CD36, and CAV1 were evaluated as genes of interest suspected to be directly bound by miR-29. Elastin, and ABHD5 are known targets of miR-29 previously demonstrated, and used as positive controls; in contrast, G6PC and HPRT were used as negative controls with regard to miR-29 direct targeting.[42, 43] More detailed information is provided in the Supplemental Information section.

Animal studies

Transgenic Mice—We used the Rosa26-rtTA2 x $TetO_7$-$Bmpr2^{R899X}$ FVB/N and Rosa26-rtTA2 x TetO7-Bmpr2(delx4+) previously described [44–46], called Rosa26-$Bmpr2^{R899X}$ and Rosa26-$Bmpr2^{delx4+}$ for brevity. The term Rosa26 is used to identify control mice without Bmpr2 mutation. R899X is an arginine to termination mutation at amino acid 899 in the BMPR2 tail domain found in family US33 and several others [47], while Rosa26-$Bmpr2^{delx4+}$ has deletion from just after the transmembrane domain onward. For both Rosa26-$Bmpr2^{R899}$X and Rosa26-Bmpr2(delx4+), expression of transgene occurs in all tissue types, but only after initiation of doxycycline. Both male and female mice were used.

For experiments on effects of 16αOHE exposure, adult Rosa26, Rosa26-Bmpr2^{R899X}, or Rosa26-Bmpr2^{delx4+} mice had the transgene activated with doxycycline at 0.2 mg/g in chow. Mice were implanted with Alzet osmotic pumps delivering either vehicle alone (polyethylene glycol) or 16αOHE at 1.25 μg/hr, which is a dose we have previously demonstrated to promote a PAH phenotype in these mice; this dose was initially demonstrated to be a dose at which 16αOHE has significant estrogenic bioactivity in murine models[22, 48]. After four weeks with osmotic pumps, the mice underwent hemodynamic profiling and were sacrificed and processed for miRNA purification.

We also performed experiments to antagonize miR-29 using an antagomir for miR-29 (α-miR-29). LNA-antimirs were synthesized by Exiqon (Vedbaek, Denmark) as an LNA-modified oligonucleotide that contained phosphorothioate backbone for use in miRNA functional studies. LNA-miR-29 was synthesized based on sequence 5′-ATTTCAAATGGTGCT-3′, which is complementary to miR-29. A scrambled oligonucleotide, LNA-Co, 5′-ACGTCTATACGCCCA-3′, was chosen according to manufacturer instructions and used as control. The scrambled oligonucleotide was chosen because it met criteria including: 3 requirements: (a) same nucleotide composition as the input sequence; (b) passed the same extensive siRNA filtering (e.g. no low complex sequence); and, (c) has the weakest (or no) match with any miRNA in the miRNA pool. LNA-antimirs were dissolved in saline and injected intravenously via tail vein into mice once a week at a dose of 20 mg/kg. After six weeks, mice underwent hemodynamic phenotyping, as described below.

All animal procedures were approved by the Institutional Animal Care and Use Committee, Vanderbilt University School of Medicine (Nashville, TN, USA).

Hemodynamic phenotyping—Two dimensional echocardiography was performed using a Vivo 770© High-Resolution Image System (VisuaSonics Toronto, Canada). Echocardiograms including B-mode, M-mode and spectral Doppler images were obtained the day prior to sacrifice under isoflurane anesthetic, as previously described[21].

Right ventricular systolic pressure (RVSP) was directly measured via insertion of a 1.4F Mikro-tip© catheter transducer (Millar Instruments Houston, TX) into a surgically exposed right internal jugular vein as previously described [47]. Pulmonary vascular resistance was calculated as (80*RVSP)/(3*CO) as previously described [47].

Immunostaining—Paraffin-embedded mouse lung sections were treated using a standard processing method for immunostaining and incubated with primary antibody smooth muscle alpha actin (SMA) (1:500; DAKO, Ft. Collins, Colo., USA) overnight followed by Alexa 488 fluorescent secondary antibody (1:500, Invitrogen, Carlsbad, Calif., USA). All antibodies were diluted in a blocking buffer (tris-buffered saline tween with 10% fetal calf serum) and controls consisted of primary isotype with secondary antibody or secondary antibody only. Quantitation of muscularization was performed by counting smooth muscle alpha actin (SMA) positive vessels per field of view in paraffin-stained lung sections.

Immunolocalization of ceramides was performed on paraffin-embedded mouse lung tissue. Lung sections were deparaffinized, rehydrated. The sections were blocked with 5% normal goat serum or 5% BSA, followed by an overnight incubation at 4°C with ceramide antibody (Enzo Life Sciences, Farmingdale, NY). Next day, the sections were incubated with biotinylated IgM secondary antibody followed by incubation with HRP-conjugated streptavidin. Diaminobenzidine (DAB) was used as a substrate for HRP (Vector Labs, Burlingame, CA). The sections were dehydrated and mounted in Cytoseal 60 (Richard-Allan Scientific, Kalamazoo, MI) for light microscopic examination.

Trichrome stain was performed on paraffin-embedded mouse lung sections. The trichrome stain reagents were purchased from Sigma-Aldrich (St. Louis, MO) and the stain was performed according to manufacturer's instructions.

Electron microscopy—For electron microscopy studies, we used murine pulmonary artery smooth muscle cells (PASMC), as well as human endothelial-like cells derived from iPS cell lines as we previously described.[49] Cells were cultured in 100 mm dishes and were subjected for LNA-miR-Co or LNA-miR-29 transfections. Twenty-four hours after transfection, the cells were fixed in 2.5% gluteraldehyde in 0.1M cacodylate buffer, at room temperature (RT) for 1 hour then transferred to 4°C, overnight.

Specimens were processed for TEM and imaged in the Vanderbilt Cell Imaging Shared Resource-Research Electron Microscope facility. Briefly, the samples were post-fixed in 1% osmium tetraoxide RT then washed 3 times with 0.1M cacodylate buffer. Subsequently, the samples were dehydrated through a graded ethanol series followed by incubation in 100% ethanol and propylene oxide (PO) and 2 exchanges of pure PO. Samples were embedded in epoxy resin and polymerized at 60°C for 48 hours. 70–80nm ultra-thin sections were then cut from the block and collected on 300-mesh copper grids. The copper grids were post-section stained at room temperature with 2% uranyl acetate and then with lead citrate. Samples were subsequently imaged on the Philips/FEI Tecnai T12 electron microscope at various magnifications.

Cells were randomly selected and pictured by a blinded observer in the electron microscopy core lab. All the mitochondria in the pictures are measured using tools from Image J, the open-sourced imaging program.

Insulin resistance measures

Insulin resistance was determined by the homeostasis model assessment of insulin resistance (HOMA-IR). This study was developed to model the dynamic interaction of insulin and glucose across a range of variations in insulin resistance and pancreatic β-cell function, and correlates well with the degree of insulin sensitivity and resistance.[50–52] The HOMA-IR uses the formula: fasting glucose (mmol/L) × fasting insulin (μU/mL)/22.5. Mouse plasma was used for studies involving the HOMA-IR assay. Studies were performed by the Hormone Assay and Analytical Services Core, Vanderbilt, Nashville, TN.

Statistics

Statistical methods for array analysis are described above. For non-array analyses with normal distribution, statistical significance was evaluated using parametric statistical techniques with two-sided testing, with a p-value of <0.05 considered statistically significant. Statistical analysis was performed using the statistical package SPSS for Windows (Version 21; IBM SPSS Statistics 21.0, Armonk, NY, USA) or JMP program (SAS, Cary, NC). Comparisons including multiple independent variables, such as mutation status and 16αOHE, or mutation status and presence of α-miR29, were performed using two-way ANOVA, with Fisher's LSD as a post-hoc test to determine the source of significance.

For principal components analysis, data was first normalized such that the average for each probe set was zero, and then the Principal Components Analysis function in JMP applied to all miR assessed by the Exiqon arrays. Eigenvectors for the first and second principal component were exported and plotted for Figures 1A and 2A. Given the nature of the study, there is no adjustment for multiple comparisons.

RESULTS

Arrays suggest disease-specific changes in miRNA expression in human PAH

miR expression arrays were used to search for differences in expression which might contribute to PAH pathogenesis, recognizing that end-stage lung disease may influence miR expression independent of PAH. Thus, Exiqon miRNA arrays were used to determine expression levels in female lungs from HPAH and control, as well as female IPF subjects (Table 1). While IPF is also a global lung disease, the pathogenesis of IPF is distinct from that of PAH using the strict phenotypic selection we employed. As a result, IPF subjects were included *a priori* as a mechanism to suggest whether any miRNA differences observed between HPAH and control lungs were: (a) a more generic result of global lung abnormality; or (b) a distinct feature of HPAH lungs not present in a separate lung disease (IPF).

The control subjects were healthy individuals who died in traumatic accidents. For each subject, two independent samples were taken, and for each disease state, a pooled set was run for comparison. Of 1439 miRNA probe sets, 196 were expressed above the noise in at least one of IPF, PAH, or control. Principal Components Analysis showed that the two samples from each patient were nearly identical, and that the two patients from each disease state clustered together closely (Figure 1A). Although the sample number is small, the low variability suggests disease-specific effect. Comparing PAH to control, there were 65 probe sets with a 95% probability of at least a 30% change (Figure 1B). These included many probe sets described as regulating metabolism (*), including the entirety of the miR29 cluster (miR29a, b, and c). Upregulation of the miR-29 cluster was confirmed by quantitative RT-PCR using RNA from control or PAH human lung (Figure 1C).

miR-29 is induced by both Bmpr2 mutation and 16αOHE in mice

We had previously published data suggesting that the primary pathogenic effect of estrogen in the context of BMPR2 mutation was related to deleterious effects on metabolism, including insulin resistance [22]. We thus wished to determine whether the estrogen metabolite 16αOHE contributed to the regulation of miRNAs known to relate to metabolism, with particular interest in the miR-29 family.

To determine whether we could use our Bmpr2 mutant murine model of pulmonary hypertension to model the miR dysregulation found in human patients, Exiqon miRNA arrays were used to determine miRNA expression levels in male Rosa26-Bmpr2^{delx4+} transgenic mice. Male mice were employed because they allow for a more direct control of estrogen exposure, so that the predominant estrogen exposure in the model system is 16αOHE. A pool of miRNA from three mice was used for each miRNA expression array to compare mice that received vehicle (n=3) to those receiving the estrogen metabolite 16αOHE (n=3) in osmotic pumps as previously described [22].

Of 1209 probe sets, 303 had expression levels above background level. Principal Components Analysis on these clearly separates the groups (Figure 2A), with the first principal component corresponding roughly to ‘Bmpr2 mutation effect’ and the second principal component corresponding to ‘16αOHE effect’, although the Bmpr2 mutant mice were already substantially moved on the ‘16αOHE effect’ axis. A heatmap of the top 50 miRNAs with altered regulation showed the same miRNA cluster 29 in a group of genes with strong upregulation by 16αOHE in control mice, and weaker upregulation in Bmpr2 mutant (Figure 2B, starred miRNA labels). This was confirmed by quantitative RT-PCR (Figure 2C), which found that the miR-29 cluster (miR-29a, miR-29b, miR-29c) had a roughly 2x higher expression in activated Bmpr2 mutant mice lungs at baseline, increasing to 4–8x upregulation with 16αOHE treatment.

Molecular markers of insulin resistance are abnormal in murine and human PAH, and influenced by the estrogen metabolite 16αOHE and miR-29

As mentioned, we recently reported a potential causal relationship between increased 16αOHE and increased PAH penetrance, including alterations in insulin-resistance related pathways.[22] Because we also recently found an association between glucocorticoid insensitivity and murine Bmpr2 PAH[21], we explored molecular markers of insulin resistance using the same mice (vehicle (n=6) versus estrogen metabolite 16αOHE (n=6)) as in the microarray experiment described above and shown in Figure 2 (male Rosa26-Bmpr2^{delx4+} transgenic mice) (Figure 3). Western blot analyses of whole mouse lung protein demonstrate that PPARγ and CD36 levels were each significantly reduced in wild-type animals exposed to 16αOHE compared to vehicle treated wild-type animals. Bmpr2 mutant animals not exposed to 16αOHE had significantly reduced PPARγ and CD36 levels compared to vehicle treated wild-type animals. Exposure of Bmpr2 mutant animals to 16αOHE further reduced both PPARγ and CD36 compared to Bmpr2 mutant animals treated with vehicle. These findings demonstrate that 16αOHE directly reduces PPARγ and CD36 levels, and the magnitude of reduction is higher in the setting of a Bmpr2 mutation (Figure 3A).

In addition, we analyzed the lung specimens from the human PAH subjects (n=2) evaluated by the whole lung miRNA array, as well as the human control subjects (n=2) in the microarray study described in Figure 1. Western blots show that PPARγ, GLUT4, and CD36 protein levels were substantially reduced in PAH patients (n=2, same as Figure 1) compared to controls (n=2, same as Figure 1) (Figure 3B).

Next, pulmonary microvascular endothelial cells (PMVECs) cultured from the male Rosa26-Bmpr2^{delx4+} transgenic mice were used to analyze *in vitro* protein production by endothelial cells. Cultured murine PMVEC from mice with the activated Bmpr2 mutation showed reduced levels of PPARγ, Glut4, and CD36 protein. These levels were further reduced by the addition of 16αOHE, consistent with the whole lung protein data (Figure 3C).

Because we suspect metabolic irregularities are not cell-specific, we believed that the mechanisms of interest would also be detectable in pulmonary vascular smooth muscle cells (PVSMC). We next hypothesized that antagonism of miR-29 would restore PPARγ and CD36 gene expression *in vitro*. Cultured mouse pulmonary vascular smooth muscle cells (PVSMC) from male Rosa26-Bmpr2^{delx4+} transgenic mice were used to assess the effect of mir-29 antagonism (α-miR-29). We first assessed the specificity of miR-29 antagonism. Metrics used were known gene targets which the miR-29 family downregulates. Addition of α-miR29 improved expression of known targets CD36, Col1a1, Eln, and Ppargc1a, but not related genes, suggesting specificity of miR-29 antagonism (Figure 3D). While alteration of gene expression is important, miRNA modulation of gene and protein expression are often not equal, particularly given that many miRNAs influence the expression of genes into proteins at the post-transcriptional level.[53] The PPARγ and CD36 protein elevations upon exposure to α-miR29 were confirmed by Western Blot. While CD36 protein was increased, PPARγ protein significantly increased 14-fold in murine SMC culture compared to control (Figure 3E).

miR-29 family members miR-29a and miR-29c directly bind to the 3′UTR of the PPARγ gene

We next sought to determine whether miR-29 family members directly bind to the PPARγ gene, which would be a mechanism by which microRNAs influence gene expression. miRNA pull-down assays suggest that the 3′UTR of the genes PPARγ and CAV1, as well as the positive controls Elastin and ABHD5, directly bind to miR-29a and miR-29c (Figure 4). miR-29b does not appear to bind to the 3′UTR of the negative control genes, as expected. In addition, the miR-29 family did not appear to bind to the 3′UTR of CD36 (Supplemental Figure 1) as miR-29a and miR-29c affinity purification did not pull down CD36 mRNA. These results suggest that PPARγ and CAV1, but not CD36, are direct targets of miR-29a and miR-29c.

Antagonism of miR-29 significantly improves hemodynamics and other features of pulmonary hypertension in a murine model of pulmonary hypertension

Transgene activated Bmpr2^{R899X} mutant mice develop an anatomic, hemodynamic, and histologic profile consistent with pulmonary hypertension; and, the penetrance is increased by 16αOHE.[22, 44, 45] We tested the hypothesis that miR-29 antagonism would prevent a

pulmonary hypertensive phenotype in a study of animals of both genders and all fed a western diet. Bmpr2^{R899X} mutant mice of both genders (n=25; female n=12, male n=13) had significantly elevated RVSP with the transgene activated compared to controls (n=13; female n=6, male n=7). Weekly injections of anti-miR-29 (αmiR-29) for 6 weeks significantly reduced RVSP among the Bmpr2^{R899X} mutation group (n=26; female n=13, male n=13) compared to controls (n=14; female n=7, male n=7), regardless of exposure to 16αOHE (squares) or vehicle (circles) (Figure 5A). Other features of the hemodynamic profile were also improved by αmiR-29 therapy. Pulmonary vascular resistance (PVR) compared to controls (n=24; female n=13, male n=11) was elevated among Bmpr2^{R899X} mutant mice without (n=11; female n=5, male n=5) and with 16αOHE (n=11 female n=7, male n=4) as previously demonstrated (no αmiR-29 exposure). Twenty-three Bmpr2^{R899X} mice were exposed to αmiR-29: 11 without 16αOHE (6 female, 5 male) and 12 with 16αOHE (6 female, 6 male). PVR was significantly reduced among the Bmpr2^{R899X} mutant mice (n=23) treated with αmiR-29 compared to those not treated with αmiR-29 (n=22); this was true for Bmpr2^{R899X} mutant mice regardless of 16αOHE exposure (Figure 5B).

In order to assess histologic changes associated with pulmonary hypertension, the extent of pulmonary arterial muscularization was assessed. Control mice had significantly fewer muscularized small (<25 μm diameter) pulmonary arteries compared to Bmpr2^{R899X} mutant mice. αmiR-29 treatment reversed increased muscularization seen in Bmpr2^{R899X} mice, but did not change muscularization in control mice (Figure 5C and 5D; each symbol is an animal; each column represents n=4 per group, with 2 females and 2 males per each group of 4). Because miR29 down regulation has been associated with renal fibrosis, careful examination of the kidneys from mice exposed to αmiR-29 treatment was conducted by a renal pathologist.[54, 55] There was no evidence of fibrosis upon careful review (Supplemental Figure 2).

Antagonism of miR-29 reverses the lung molecular phenotype suggestive of insulin resistance

Whole lung from Bmpr2^{R899X} mutant mice have reduced PPARγ and CD36 protein levels compared to controls. Weekly αmiR-29 treatment resulted in a significant increase in PPARγ and CD36 protein in both the control and Bmpr2^{R899X} mutant mice (Figure 6A). In addition, HOMA-IR is elevated among Bmpr2^{R899X} mutant mice. Control and Bmpr2^{R899X} mutant mice treated with αmiR-29 have a significant reduction in HOMA-IR; among Bmpr2^{R899X} mutant mice the level returns to that of controls (Figure 6B). We recently reported evidence for increased synthesis and deposition of ceramide associated with the pulmonary hypertension phenotype in Bmpr2^{R899X} mutant mice, and sought to assess ceramide in the lungs with and without αmiR-29 treatment.[19] Ceramide is a key mediator of lipotoxicity elevated in the setting of insulin resistance.[56] As expected, ceramide appeared elevated in the pulmonary vasculature of Bmpr2^{R899X} mutant mice compared to controls; and, αmiR-29 treatment substantially reduced ceramide accumulation consistent with an improvement in the molecular phenotype of insulin resistance (Figure 6C).

α-miR29 treatment increases average mitochondrial size

Our group and others have been interested in the contribution of mitochondrial abnormalities to pulmonary hypertension, and we previously showed that the global expression of a Bmpr2 mutation is sufficient to cause metabolic stress and mitochondrial oxidant injury, including excess production of mitochondrial-derived reactive oxygen species (ROS).[1, 20, 25, 57–59] This, in concert with the emerging appreciation that mitochondrial morphology is a dynamic process but that larger mitochondria may indicate reduced fission and associate with better outcomes in PAH, we sought to assess mitochondrial morphology with and without miRNA-29 antagonism.[25, 60] One mechanism by which miRNA-29 antagonism may correct energy metabolic problems is through the regulation of mitochondrial fission and fusion; the contribution of mitochondrial dynamics to pulmonary vascular disease and right ventricular response to stress are of great interest in the field.[61] The regulation of mitochondrial fission and fusion may occur via Ppargc1a or PPARγ increase[62], as suggested by Figures 3E and 3D. We tested this by measuring the size of mitochondria in pulmonary artery smooth muscle cells derived from mice treated with the α-miR29 antagomir or vehicle (Supplement Figure 2, Figures 2A and 2B). miRNA-29 inhibition increased the long axis of mitochondria (7A, 7B, 7C; Supplement Figure 2, Figure 2C). Because an electron micrograph is a two dimensional section through a three-dimensional object, this probably understates the resolution of mitochondrial hyperfissioning; if the mitochondria are randomly oriented, we might expect for some to appear nearly circular (~175 nM in both dimensions), and some to have great length. Figures 7B and 7C provide visual examples of vehicle- or α-miR29- treated PASMC, with mitochondrial long axes marked by arrows. Counts of mitochondria which appear more than twice as long as they are wide (long axis > 400 nM) are low in vehicle-treated PASMCs (8/160 (5%)) compared to those treated with α-miR29 (56/177 (32%))—this is a six-fold increase ($p<.0001$ by Pearson Chi Square). Variation in mitochondrial size was more than doubled, with standard deviation from the median 104 nM in vehicle-treated compared to 230 nM in α-miR29 treated PASMC cells ($p<.0001$ by Brown-Forsythe) (Figures 7B and 7C; Supplement Figure 2, Figures 2D and 2E).

We further assessed mitochondrial size using endothelial-like cells derived from human subjects. Specifically, we used induced pluripotent stem cells (iPS) derived a healthy control subject as well as from a patient with *BMPR2*-mutation associated HPAH to derive endothelial-like cells for mitochondrial evaluation. Overall, mitochondria from healthy control endothelial-like cells were larger and more variable in size than mitochondria from HPAH patient endothelial-like cells. For both groups, treatment with α-miR29 increased mitochondrial size (Figures 7F, 7E, 7G)

DISCUSSION

In these experiments, we used human lung tissue and transgenic mouse models of mutant Bmpr2 to demonstrate that increased expression of miR-29 family is a shared feature of human and murine-modeled HPAH. We further demonstrate that functional and molecular markers of insulin resistance are abnormal in HPAH, and this effect is amplified by the estrogen metabolite 16αOHE as well as associated with elevated miR-29. Furthermore, in

the setting of 16αOHE exposure, we demonstrate a beneficial effect of miR-29 antagonism in terms of disease penetrance, hemodynamics, and pulmonary histopathology in our murine model. While correcting the pulmonary hypertension phenotype, treatment with αmiR29 also improved indices of insulin resistance and metabolic dysregulation, as well as mitochondrial morphology. In summary, these findings support the concept that 16αOHE contributes to HPAH pathogenesis in the setting of a BMPR2 mutation, and suggest that miR-29 antagonism may provide a novel therapeutic approach for HPAH.

Among the many perplexing features of human PAH, including HPAH, are the cell-level markers of altered energy metabolism as well as the systemic features of female predominance and the association of PAH with insulin resistance and the metabolic syndrome. Independent of PAH, sex hormones are associated with insulin resistance and abnormalities of energy metabolism, which may provide some clues as to how gender and metabolism interface. For example, in women both subphysiologic and supraphysiologic estrogen levels associate with insulin resistance and type 2 diabetes mellitus; but, in men the association is strongest with high estrogen and low testosterone levels.[63–66] However, these findings do not provide the precise mechanistic link between sex hormones, cellular and systemic metabolic abnormalities and PAH. MicroRNAs (miRNAs; miRs) are short, single-stranded non-protein coding gene products typically 20–22 nucleotides in length that post-transcriptionally regulate the expression of target genes through interactions with specific mRNAs.[67–69] There is certainly a growing recognition of the role miRNAs play in cardiopulmonary diseases, including PAH.[70–78] Our finding on tissue microRNA arrays from HPAH patients and Bmpr2 transgenic mice showed a consistent pattern of microRNAs distinct from controls. The patterns were also consistent with previous studies related to insulin resistance and metabolic derangements, including a significant and consistent elevation of miR-29 family expression.[32, 79] Our subsequent studies demonstrated a molecular fingerprint consistent with insulin resistance and metabolic derangements which was attenuated by miR-29 antagonism in concert with hemodynamic improvement and improvement in the physiologic HOMA-IR metric of insulin resistance. While requiring replication, our results suggest that miR-29 contributes to HPAH pathogenesis, at least in the setting of an elevated 16αOHE. We previously demonstrated that female and male HPAH patients have an estrogen milieu that is skewed toward higher levels of 16αOHE, and believe that this skewed sex hormone metabolism results in miR29 upregulation in HPAH.[12, 22] 16αOHE binds to the estrogen receptors with high affinity, and we suspect that canonical signaling via estrogen receptor α and/or estrogen receptor β promotes enhances miR29 expression.[80] Importantly, our findings in the murine model did not differentiate according to sex, although mice of both sex received exogenous 16αOHE in this study.

Our work has similarities and differences to recent work by Mair and colleagues that demonstrated the beneficial effect of estrogen antagonism to attenuate PH in female murine models. Unlike the current study, they found that while female disease was attenuated, there was insufficient effect in the male subgroup.[8] This may be due to the naturally lower circulating levels of estrogens in males rather than an inherent inability of males to respond to estrogen antagonism; in our model mice of both sex were exogenously exposed to the estrogenic compound 16αOHE. They also found reduced lung aromatase levels in both cultured PASMCs and the pulmonary artery smooth muscle cell layer in the male animals

compared to females. This finding suggests an organ-specific phenomenon related to local estrogen production and metabolism is also possible. While we found no difference in murine PASMC mitochondrial size according to sex, association of mitochondrial fragmentation and dysmorphology with local aromatase activity would be an area for future study.

We previously demonstrated that 16αOHE not only associates with human female HPAH in BMPR2 mutants, but also amplifies HPAH penetrance and phenotype among Bmpr2 transgenic mice of both genders.[22] Our current study is unique in that we identify a potential molecular mechanism for this effect: miR-29 promotion of metabolic derangements known to associate with HPAH and IPAH, including insulin resistance and alterations in lipid metabolism.[19, 26–30] Increased ceramide in the lungs suggest impairment of the fatty acid oxidation pathway. Consistent with this, we previously reported endothelial cells with BMPR2 mutations have reduced expression of genes involved in fatty acid oxidation.[20] miR-29 appears to be a critical node in the network of factors associated with glucose and lipid homeostasis, with regulatory roles linked to insulin secretion as well as the regulation of key lipid metabolizing genes.[31, 81–83] Our data suggesting a link between the estrogen metabolite 16αOHE and miR-29 is novel in HPAH, although estradiol has previously been shown to induce miR-29 expression in a murine model of hepatic injury.[84]

Our study had several limitations that warrant discussion. While the subsequent findings presented suggest that elevated miR-29 is a feature of HPAH, the initial discovery of miR-29 elevation was made using a small number of specimens studied using an array platform which could result in false positive results. In addition, the manner by which 16αOHE increases miR-29 will be an opportunity for future study, although previous work suggests that the suppression of the nuclear factor-κB (NF-κB) signaling pathway contributes.[84] Other mechanisms that promote derangements in energy metabolism, including how glucose flux and insulin resistance influences pulmonary vascular signaling in the human BMPR2 and mouse Bmpr2 mutant conditions are not addressed by these studies and will be areas for future study. While our studies suggest a direct effect of miR-29 on PPARγ expression and energy metabolism, we recognize that alternative results from miR-29 activity which may be pathogenic are possible. In addition, it is notable that miR-29 antagonism improved CD36 and GLUT4 levels despite an absence of data to suggest direct binding of miR-29 to the 3′UTR of those genes; we suspect that this supports the growing body of literature suggestive that PPARγ directly regulates CD36 and GLUT4, but this requires further study.[85, 86] Furthermore, while reduced BMP signaling appears to be a central feature of many PAH forms, the work presented specifically concerns BMPR2-associated HPAH; whether or not these findings are directly applicable to other forms of PAH will need to be explored. Finally, we recognize the complexity of sex hormone associations with regard to the heart adaptation to stress are not addressed by these studies; this may be particularly relevant given the growing concern that while females develop PAH more often, they also appear to live longer after diagnosis than males.[28, 87, 88] Finally, our findings will require exploration in other animal models representative of PAH.

In conclusion, we demonstrate a potential mechanism by which 16αOHE promotes HPAH, with the finding of elevated miR-29 in human lung tissue from female patients with HPAH.

We confirmed the presence of miR-29 family upregulation in a murine model of PAH using an exogenous estrogen metabolite (16αOHE) applied to animals with mutant Bmpr2 expression. Further, the deleterious effects of a 16αOHE, including the PAH phenotype, were attenuated by direct antagonism of miR-29. Coincident with phenotypic improvement, molecular and functional indices of deranged energy metabolism were attenuated by miR-29 antagonism despite continued exposure to 16αOHE. While further studies of the precise mechanism by which antagonism of miR-29 attenuates the HPAH phenotype and molecular alterations is warranted, novel therapeutic approaches to treat PAH without the complication of direct sex hormone modification may emerge.

Supplementary Material

Refer to Web version on PubMed Central for supplementary material.

Acknowledgments

The authors thank the subjects and families who graciously contributed to this work.

Funding Sources: Funding was provided by NIH P01 HL 108800, NIH K08 HL 093363 (Hemnes), and NIH K23 HL 098743, as well as by the Entelligence Young Investigators Award Program. The project was also supported by CTSA award No. UL1TR000445 from the National Center for Advancing Translational Sciences.

References

1. Tuder RM, Archer SL, Dorfmuller P, Erzurum SC, Guignabert C, Michelakis E, Rabinovitch M, Schermuly R, Stenmark KR, Morrell NW. Relevant issues in the pathology and pathobiology of pulmonary hypertension. J Am Coll Cardiol. 2013; 62:D4–12. [PubMed: 24355640]
2. Austin ED, Lahm T, West J, Tofovic SP, Johansen AK, Maclean MR, Alzoubi A, Oka M. Gender, sex hormones and pulmonary hypertension. Pulm Circ. 2013; 3:294–314. [PubMed: 24015330]
3. Austin ED, Loyd JE. The genetics of pulmonary arterial hypertension. Circ Res. 2014; 115:189–202. [PubMed: 24951767]
4. Chin KM, Rubin LJ. Pulmonary arterial hypertension. J Am Coll Cardiol. 2008; 51:1527–38. [PubMed: 18420094]
5. Humbert M, Sitbon O, Chaouat A, Bertocchi M, Habib G, Gressin V, Yaici A, Weitzenblum E, Cordier JF, Chabot F, Dromer C, Pison C, Reynaud-Gaubert M, Haloun A, Laurent M, Hachulla E, Simonneau G. Pulmonary arterial hypertension in France: results from a national registry. Am J Respir Crit Care Med. 2006; 173:1023–30. [PubMed: 16456139]
6. Badesch DB, Raskob GE, Elliott CG, Krichman AM, Farber HW, Frost AE, Barst RJ, Benza RL, Liou TG, Turner M, Giles S, Feldkircher K, Miller DP, McGoon MD. Pulmonary arterial hypertension: baseline characteristics from the REVEAL Registry. Chest. 2010; 137:376–87. [PubMed: 19837821]
7. Humbert M, Sitbon O, Chaouat A, Bertocchi M, Habib G, Gressin V, Yaici A, Weitzenblum E, Cordier JF, Chabot F, Dromer C, Pison C, Reynaud-Gaubert M, Haloun A, Laurent M, Hachulla E, Cottin V, Degano B, Jais X, Montani D, Souza R, Simonneau G. Survival in patients with idiopathic, familial, and anorexigen-associated pulmonary arterial hypertension in the modern management era. Circulation. 2010; 122:156–63. [PubMed: 20585011]
8. Mair KM, Wright AF, Duggan N, Rowlands DJ, Hussey MJ, Roberts S, Fullerton J, Nilsen M, Loughlin L, Thomas M, MacLean MR. Sex-dependent influence of endogenous estrogen in pulmonary hypertension. Am J Respir Crit Care Med. 2014; 190:456–67. [PubMed: 24956156]
9. White K, Johansen AK, Nilsen M, Ciuclan L, Wallace E, Paton L, Campbell A, Morecroft I, Loughlin L, McClure JD, Thomas M, Mair KM, Maclean MR. Activity of the Estrogen-Metabolizing Enzyme Cytochrome P450 1B1 Influences the Development of Pulmonary Arterial Hypertension. Circulation. 2012; 126:1087–98. [PubMed: 22859684]

10. White K, Dempsie Y, Nilsen M, Wright AF, Loughlin L, MacLean MR. The serotonin transporter, gender, and 17beta oestradiol in the development of pulmonary arterial hypertension. Cardiovasc Res. 2011; 90:373–82. [PubMed: 21177701]
11. Dempsie Y, MacRitchie NA, White K, Morecroft I, Wright AF, Nilsen M, Loughlin L, Mair KM, MacLean MR. Dexfenfluramine and the oestrogen-metabolizing enzyme CYP1B1 in the development of pulmonary arterial hypertension. Cardiovasc Res. 2013; 99:24–34. [PubMed: 23519266]
12. Austin ED, Cogan JD, West JD, Hedges LK, Hamid R, Dawson EP, Wheeler LA, Parl FF, Loyd JE, Phillips JA 3rd. Alterations in oestrogen metabolism: implications for higher penetrance of familial pulmonary arterial hypertension in females. Eur Respir J. 2009; 34:1093–9. [PubMed: 19357154]
13. Roberts KE, Fallon MB, Krowka MJ, Brown RS, Trotter JF, Peter I, Tighiouart H, Knowles JA, Rabinowitz D, Benza RL, Badesch DB, Taichman DB, Horn EM, Zacks S, Kaplowitz N, Kawut SM. Pulmonary Vascular Complications of Liver Disease Study, G. Genetic risk factors for portopulmonary hypertension in patients with advanced liver disease. Am J Respir Crit Care Med. 2009; 179:835–42. [PubMed: 19218192]
14. West J, Cogan J, Geraci M, Robinson L, Newman J, Phillips JA, Lane K, Meyrick B, Loyd J. Gene expression in BMPR2 mutation carriers with and without evidence of Pulmonary Arterial Hypertension suggests pathways relevant to disease penetrance. BMC Med Genomics. 2008; 1:45. [PubMed: 18823550]
15. Sweeney L, Voelkel NF. Estrogen exposure, obesity and thyroid disease in women with severe pulmonary hypertension. Eur J Med Res. 2009; 14:433–42. [PubMed: 19748850]
16. Hankinson SE, Manson JE, Spiegelman D, Willett WC, Longcope C, Speizer FE. Reproducibility of plasma hormone levels in postmenopausal women over a 2–3-year period. Cancer Epidemiol Biomarkers Prev. 1995; 4:649–54. [PubMed: 8547832]
17. Simpson ER, Mahendroo MS, Means GD, Kilgore MW, Corbin CJ, Mendelson CR. Tissue-specific promoters regulate aromatase cytochrome P450 expression. J Steroid Biochem Mol Biol. 1993; 44:321–30. [PubMed: 8476746]
18. West J, Cogan J, Geraci M, Robinson L, Newman J, Phillips JA, Lane K, Meyrick B, Loyd J. Gene expression in BMPR2 mutation carriers with and without evidence of pulmonary arterial hypertension suggests pathways relevant to disease penetrance. BMC Med Genomics. 2008; 1:45. [PubMed: 18823550]
19. Hemnes AR, Brittain EL, Trammell AW, Fessel JP, Austin ED, Penner N, Maynard KB, Gleaves L, Talati M, Absi T, Disalvo T, West J. Evidence for right ventricular lipotoxicity in heritable pulmonary arterial hypertension. Am J Respir Crit Care Med. 2014; 189:325–34. [PubMed: 24274756]
20. Fessel JP, Flynn CR, Robinson LJ, Penner NL, Gladson S, Kang CJ, Wasserman DH, Hemnes AR, West JD. Hyperoxia synergizes with mutant bone morphogenic protein receptor 2 to cause metabolic stress, oxidant injury, and pulmonary hypertension. Am J Respir Cell Mol Biol. 2013; 49:778–87. [PubMed: 23742019]
21. West J, Niswender KD, Johnson JA, Pugh ME, Gleaves L, Fessel JP, Hemnes AR. A potential role for insulin resistance in experimental pulmonary hypertension. Eur Respir J. 2013; 41:861–71. [PubMed: 22936709]
22. Fessel JP, Chen X, Frump A, Gladson S, Blackwell T, Kang C, Johnson J, Loyd JE, Hemnes A, Austin E, West J. Interaction between bone morphogenetic protein receptor type 2 and estrogenic compounds in pulmonary arterial hypertension. Pulm Circ. 2013; 3:564–77. [PubMed: 24618541]
23. Caja S, Puerta M. Control by reproduction-related hormones of resistin expression and plasma concentration. Hormone Metab Res. 2007; 39:501–6.
24. Lee MJ, Lin H, Liu CW, Wu MH, Liao WJ, Chang HH, Ku HC, Chien YS, Ding WH, Kao YH. Octylphenol stimulates resistin gene expression in 3T3-L1 adipocytes via the estrogen receptor and extracellular signal-regulated kinase pathways. Am J Physiol Cell Physiol. 2008; 294:C1542–51. [PubMed: 18417718]
25. Marsboom G, Toth PT, Ryan JJ, Hong Z, Wu X, Fang YH, Thenappan T, Piao L, Zhang HJ, Pogoriler J, Chen Y, Morrow E, Weir EK, Rehman J, Archer SL. Dynamin-related protein 1-mediated mitochondrial mitotic fission permits hyperproliferation of vascular smooth muscle cells

and offers a novel therapeutic target in pulmonary hypertension. Circ Res. 2012; 110:1484–97. [PubMed: 22511751]

26. Fessel JP, Hamid R, Wittmann BM, Robinson LJ, Blackwell T, Tada Y, Tanabe N, Tatsumi K, Hemnes AR, West JD. Metabolomic analysis of bone morphogenetic protein receptor type 2 mutations in human pulmonary endothelium reveals widespread metabolic reprogramming. Pulm Circ. 2012; 2:201–13. [PubMed: 22837861]
27. Hansmann G, Wagner RA, Schellong S, Perez VA, Urashima T, Wang L, Sheikh AY, Suen RS, Stewart DJ, Rabinovitch M. Pulmonary arterial hypertension is linked to insulin resistance and reversed by peroxisome proliferator-activated receptor-gamma activation. Circulation. 2007; 115:1275–84. [PubMed: 17339547]
28. Zamanian RT, Hansmann G, Snook S, Lilienfeld D, Rappaport KM, Reaven GM, Rabinovitch M, Doyle RL. Insulin resistance in pulmonary arterial hypertension. Eur Respir J. 2009; 33:318–24. [PubMed: 19047320]
29. Pugh ME, Robbins IM, Rice TW, West J, Newman JH, Hemnes AR. Unrecognized glucose intolerance is common in pulmonary arterial hypertension. J Heart Lung Transplant. 2011; 30:904–11. [PubMed: 21493097]
30. Sutendra G, Bonnet S, Rochefort G, Haromy A, Folmes KD, Lopaschuk GD, Dyck JR, Michelakis ED. Fatty acid oxidation and malonyl-CoA decarboxylase in the vascular remodeling of pulmonary hypertension. Sci Transl Med. 2010; 2:44ra58.
31. Bagge A, Clausen TR, Larsen S, Ladefoged M, Rosenstierne MW, Larsen L, Vang O, Nielsen JH, Dalgaard LT. MicroRNA-29a is up-regulated in beta-cells by glucose and decreases glucose-stimulated insulin secretion. Biochem Biophys Res Commun. 2012; 426:266–72. [PubMed: 22940552]
32. Kurtz CL, Peck BC, Fannin EE, Beysen C, Miao J, Landstreet SR, Ding S, Turaga V, Lund PK, Turner S, Biddinger SB, Vickers KC, Sethupathy P. microRNA-29 fine-tunes the expression of key FOXA2-activated lipid metabolism genes and is dysregulated in animal models of insulin resistance and diabetes. Diabetes. 2014; 63:3141–8. Epub 2014 Apr 10. 10.2337/db13-1015 [PubMed: 24722248]
33. Simonneau G, Gatzoulis MA, Adatia I, Celermajer D, Denton C, Ghofrani A, Gomez Sanchez MA, Krishna Kumar R, Landzberg M, Machado RF, Olschewski H, Robbins IM, Souza R. Updated clinical classification of pulmonary hypertension. J Am Coll Cardiol. 2013; 62:D34–41. [PubMed: 24355639]
34. Raghu G, Collard HR, Egan JJ, Martinez FJ, Behr J, Brown KK, Colby TV, Cordier JF, Flaherty KR, Lasky JA, Lynch DA, Ryu JH, Swigris JJ, Wells AU, Ancochea J, Bouros D, Carvalho C, Costabel U, Ebina M, Hansell DM, Johkoh T, Kim DS, King TE Jr, Kondoh Y, Myers J, Muller NL, Nicholson AG, Richeldi L, Selman M, Dudden RF, Griss BS, Protzko SL, Schunemann HJ. An official ATS/ERS/JRS/ALAT statement: idiopathic pulmonary fibrosis: evidence-based guidelines for diagnosis and management. Am J Respir Crit Care Med. 2011; 183:788–824. [PubMed: 21471066]
35. Ritchie ME, Silver J, Oshlack A, Holmes M, Diyagama D, Holloway A, Smyth GK. A comparison of background correction methods for two-colour microarrays. Bioinformatics. 2007; 23:2700–7. [PubMed: 17720982]
36. Chang CC, Lin CC, Hsieh WL, Lai HW, Tsai CH, Cheng YW. MicroRNA expression profiling in PBMCs: a potential diagnostic biomarker of chronic hepatitis C. Disease Markers. 2014; 2014:367157. [PubMed: 25505813]
37. Lv LL, Cao YH, Ni HF, Xu M, Liu D, Liu H, Chen PS, Liu BC. MicroRNA-29c in urinary exosome/microvesicle as a biomarker of renal fibrosis. Am J Physiol Renal Physiol. 2013; 305:F1220–7. [PubMed: 23946286]
38. Orom UA, Lund AH. Experimental identification of microRNA targets. Gene. 2010; 451:1–5. [PubMed: 19944134]
39. Orom UA, Lund AH. Isolation of microRNA targets using biotinylated synthetic microRNAs. Methods. 2007; 43:162–5. [PubMed: 17889804]
40. Kedde M, Strasser MJ, Boldajipour B, Oude Vrielink JA, Slanchev K, le Sage C, Nagel R, Voorhoeve PM, van Duijse J, Orom UA, Lund AH, Perrakis A, Raz E, Agami R. RNA-binding

protein Dnd1 inhibits microRNA access to target mRNA. Cell. 2007; 131:1273–86. [PubMed: 18155131]

41. Orom UA, Nielsen FC, Lund AH. MicroRNA-10a binds the 5′UTR of ribosomal protein mRNAs and enhances their translation. Mol Cell. 2008; 30:460–71. [PubMed: 18498749]
42. Ott CE, Grunhagen J, Jager M, Horbelt D, Schwill S, Kallenbach K, Guo G, Manke T, Knaus P, Mundlos S, Robinson PN. MicroRNAs differentially expressed in postnatal aortic development downregulate elastin via 3′ UTR and coding-sequence binding sites. PLoS ONE. 2011; 6:e16250. [PubMed: 21305018]
43. Kurtz CL, Peck BC, Fannin EE, Beysen C, Miao J, Landstreet SR, Ding S, Turaga V, Lund PK, Turner S, Biddinger SB, Vickers KC, Sethupathy P. MicroRNA-29 fine-tunes the expression of key FOXA2-activated lipid metabolism genes and is dysregulated in animal models of insulin resistance and diabetes. Diabetes. 2014; 63:3141–8. [PubMed: 24722248]
44. Yasuda T, Tada Y, Tanabe N, Tatsumi K, West J. Rho-kinase inhibition alleviates pulmonary hypertension in transgenic mice expressing a dominant-negative type II bone morphogenetic protein receptor gene. Am J Physiol Lung Cell Mol Physiol. 2011; 301:L667–74. [PubMed: 21856816]
45. Johnson JA, Hemnes AR, Perrien DS, Schuster M, Robinson LJ, Gladson S, Loibner H, Bai S, Blackwell TR, Tada Y, Harral JW, Talati M, Lane KB, Fagan KA, West J. Cytoskeletal defects in Bmpr2-associated pulmonary arterial hypertension. Am J Physiol Lung Cell Mol Physiol. 2012; 302:L474–84. [PubMed: 22180660]
46. West J, Fagan K, Steudel W, Fouty B, Lane K, Harral J, Hoedt-Miller M, Tada Y, Ozimek J, Tuder R, Rodman DM. Pulmonary hypertension in transgenic mice expressing a dominant-negative BMPRII gene in smooth muscle. Circ Res. 2004; 94:1109–14. [PubMed: 15031260]
47. West J, Harral J, Lane K, Deng Y, Ickes B, Crona D, Albu S, Stewart D, Fagan K. Mice expressing BMPR2R899X transgene in smooth muscle develop pulmonary vascular lesions. Am J Physiol Lung Cell Mol Physiol. 2008; 295:L744–55. [PubMed: 18723761]
48. Lustig RH, Mobbs CV, Bradlow HL, McEwen BS, Pfaff DW. Differential effects of estradiol and 16 alpha-hydroxyestrone on pituitary and preoptic estrogen receptor regulation. Endocrinology. 1989; 125:2701–9. [PubMed: 2792004]
49. West JD, Austin ED, Gaskill C, Marriott S, Baskir R, Bilousova G, Jean JC, Hemnes AR, Menon S, Bloodworth NC, Fessel JP, Kropski JA, Irwin D, Ware LB, Wheeler L, Hong CC, Meyrick B, Loyd JE, Bowman AB, Ess KC, Klemm DJ, Young PP, Merryman WD, Kotton D, Majka SM. Identification of a common Wnt-associated genetic signature across multiple cell types in pulmonary arterial hypertension. Am J Physiol Cell Physiol. 2014; 307:C415–30. [PubMed: 24871858]
50. Matthews DR, Hosker JP, Rudenski AS, Naylor BA, Treacher DF, Turner RC. Homeostasis model assessment: insulin resistance and beta-cell function from fasting plasma glucose and insulin concentrations in man. Diabetologia. 1985; 28:412–9. [PubMed: 3899825]
51. Muniyappa R, Lee S, Chen H, Quon MJ. Current approaches for assessing insulin sensitivity and resistance in vivo: advantages, limitations, and appropriate usage. Am J Physiol Endocrinol Metab. 2008; 294:E15–26. [PubMed: 17957034]
52. Radziuk J. Insulin sensitivity and its measurement: structural commonalities among the methods. J Clin Endocrinol Metab. 2000; 85:4426–33. [PubMed: 11134088]
53. Hudson WH, Ortlund EA. The structure, function and evolution of proteins that bind DNA and RNA. Nat Rev Mol Cell Biol. 2014; 15:749–60. [PubMed: 25269475]
54. Qin W, Chung AC, Huang XR, Meng XM, Hui DS, Yu CM, Sung JJ, Lan HY. TGF-beta/Smad3 signaling promotes renal fibrosis by inhibiting miR-29. J Am Soc Nephrol. 2011; 22:1462–74. [PubMed: 21784902]
55. Wang B, Komers R, Carew R, Winbanks CE, Xu B, Herman-Edelstein M, Koh P, Thomas M, Jandeleit-Dahm K, Gregorevic P, Cooper ME, Kantharidis P. Suppression of microRNA-29 expression by TGF-beta1 promotes collagen expression and renal fibrosis. J Am Soc Nephrol. 2012; 23:252–65. [PubMed: 22095944]

56. Long SD, Pekala PH. Lipid mediators of insulin resistance: ceramide signalling down-regulates GLUT4 gene transcription in 3T3-L1 adipocytes. Biochem J. 1996; 319(Pt 1):179–84. [PubMed: 8870666]
57. Archer SL, Gomberg-Maitland M, Maitland ML, Rich S, Garcia JG, Weir EK. Mitochondrial metabolism, redox signaling, and fusion: a mitochondria-ROS-HIF-1alpha-Kv1.5 O2-sensing pathway at the intersection of pulmonary hypertension and cancer. Am J Physiol Heart Circ Physiol. 2008; 294:H570–8. [PubMed: 18083891]
58. Rehman J, Archer SL. A proposed mitochondrial-metabolic mechanism for initiation and maintenance of pulmonary arterial hypertension in fawn-hooded rats: the Warburg model of pulmonary arterial hypertension. Adv Exp Med Biol. 2010; 661:171–85. [PubMed: 20204730]
59. Xu W, Koeck T, Lara AR, Neumann D, DiFilippo FP, Koo M, Janocha AJ, Masri FA, Arroliga AC, Jennings C, Dweik RA, Tuder RM, Stuehr DJ, Erzurum SC. Alterations of cellular bioenergetics in pulmonary artery endothelial cells. Proc Natl Acad Sci U S A. 2007; 104:1342–7. [PubMed: 17227868]
60. Ong SB, Hausenloy DJ. Mitochondrial morphology and cardiovascular disease. Cardiovasc Res. 2010; 88:16–29. [PubMed: 20631158]
61. Archer SL. Mitochondrial dynamics--mitochondrial fission and fusion in human diseases. N Engl J Med. 2013; 369:2236–51. [PubMed: 24304053]
62. Zolezzi JM, Silva-Alvarez C, Ordenes D, Godoy JA, Carvajal FJ, Santos MJ, Inestrosa NC. Peroxisome proliferator-activated receptor (PPAR) gamma and PPARalpha agonists modulate mitochondrial fusion-fission dynamics: relevance to reactive oxygen species (ROS)-related neurodegenerative disorders? PLoS ONE. 2013; 8:e64019. [PubMed: 23675519]
63. Cagnacci A, Soldani R, Carriero PL, Paoletti AM, Fioretti P, Melis GB. Effects of low doses of transdermal 17 beta-estradiol on carbohydrate metabolism in postmenopausal women. J Clin Endocrinol Metab. 1992; 74:1396–400. [PubMed: 1317387]
64. Godsland IF, Walton C, Felton C, Proudler A, Patel A, Wynn V. Insulin resistance, secretion, and metabolism in users of oral contraceptives. J Clin Endocrinol Metab. 1992; 74:64–70. [PubMed: 1530790]
65. Watanabe RM, Azen CG, Roy S, Perlman JA, Bergman RN. Defects in carbohydrate metabolism in oral contraceptive users without apparent metabolic risk factors. J Clin Endocrinol Metab. 1994; 79:1277–83. [PubMed: 7962320]
66. de Lauzon-Guillain B, Fournier A, Fabre A, Simon N, Mesrine S, Boutron-Ruault MC, Balkau B, Clavel-Chapelon F. Menopausal hormone therapy and new-onset diabetes in the French Etude Epidemiologique de Femmes de la Mutuelle Generale de l'Education Nationale (E3N) cohort. Diabetologia. 2009; 52:2092–100. [PubMed: 19629429]
67. Lagos-Quintana M, Rauhut R, Lendeckel W, Tuschl T. Identification of novel genes coding for small expressed RNAs. Science. 2001; 294:853–8. [PubMed: 11679670]
68. Bartel DP. MicroRNAs: genomics, biogenesis, mechanism, and function. Cell. 2004; 116:281–97. [PubMed: 14744438]
69. Koch L. Epigenetics: an epigenetic twist on the missing heritability of complex traits. Nat Rev Genet. 2014; 15:218.
70. Courboulin A, Paulin R, Giguere NJ, Saksouk N, Perreault T, Meloche J, Paquet ER, Biardel S, Provencher S, Cote J, Simard MJ, Bonnet S. Role for miR-204 in human pulmonary arterial hypertension. J Exp Med. 2011; 208:535–48. [PubMed: 21321078]
71. Kim J, Kang Y, Kojima Y, Lighthouse JK, Hu X, Aldred MA, McLean DL, Park H, Comhair SA, Greif DM, Erzurum SC, Chun HJ. An endothelial apelin-FGF link mediated by miR-424 and miR-503 is disrupted in pulmonary arterial hypertension. Nat Med. 2013; 19:74–82. [PubMed: 23263626]
72. Drake KM, Zygmunt D, Mavrakis L, Harbor P, Wang L, Comhair SA, Erzurum SC, Aldred MA. Altered MicroRNA processing in heritable pulmonary arterial hypertension: an important role for Smad-8. Am J Respir Crit Care Med. 2011; 184:1400–8. [PubMed: 21920918]
73. Caruso P, Dempsie Y, Stevens HC, McDonald RA, Long L, Lu R, White K, Mair KM, McClure JD, Southwood M, Upton P, Xin M, van Rooij E, Olson EN, Morrell NW, MacLean MR, Baker

AH. A role for miR-145 in pulmonary arterial hypertension: evidence from mouse models and patient samples. Circ Res. 2012; 111:290–300. [PubMed: 22715469]

74. Parikh VN, Jin RC, Rabello S, Gulbahce N, White K, Hale A, Cottrill KA, Shaik RS, Waxman AB, Zhang YY, Maron BA, Hartner JC, Fujiwara Y, Orkin SH, Haley KJ, Barabasi AL, Loscalzo J, Chan SY. MicroRNA-21 integrates pathogenic signaling to control pulmonary hypertension: results of a network bioinformatics approach. Circulation. 2012; 125:1520–32. [PubMed: 22371328]
75. Jalali S, Ramanathan GK, Parthasarathy PT, Aljubran S, Galam L, Yunus A, Garcia S, Cox RR Jr, Lockey RF, Kolliputi N. Mir-206 regulates pulmonary artery smooth muscle cell proliferation and differentiation. PLoS ONE. 2012; 7:e46808. [PubMed: 23071643]
76. Wang D, Zhang H, Li M, Frid MG, Flockton AR, McKeon BA, Yeager ME, Fini MA, Morrell NW, Pullamsetti SS, Velegala S, Seeger W, McKinsey TA, Sucharov CC, Stenmark KR. MicroRNA-124 controls the proliferative, migratory, and inflammatory phenotype of pulmonary vascular fibroblasts. Circ Res. 2014; 114:67–78. [PubMed: 24122720]
77. Rhodes CJ, Wharton J, Boon RA, Roexe T, Tsang H, Wojciak-Stothard B, Chakrabarti A, Howard LS, Gibbs JS, Lawrie A, Condliffe R, Elliot CA, Kiely DG, Huson L, Ghofrani HA, Tiede H, Schermuly R, Zeiher AM, Dimmeler S, Wilkins MR. Reduced microRNA-150 is associated with poor survival in pulmonary arterial hypertension. Am J Respir Crit Care Med. 2013; 187:294–302. [PubMed: 23220912]
78. Paulin R, Sutendra G, Gurtu V, Dromparis P, Haromy AS, Provencher S, Bonnet S, Michelakis ED. A miR-208-Mef2 Axis Drives the De-Compensation of Right Ventricular Function in Pulmonary Hypertension. Circ Res. 2015; 116:56–69. Epub 2014 Oct 6. 10.1161/CIRCRESAHA.115.303910 [PubMed: 25287062]
79. Rask-Madsen C, King GL. Vascular complications of diabetes: mechanisms of injury and protective factors. Cell Metab. 2013; 17:20–33. [PubMed: 23312281]
80. Swaneck GE, Fishman J. Covalent binding of the endogenous estrogen 16 alpha-hydroxyestrone to estradiol receptor in human breast cancer cells: characterization and intranuclear localization. Proc Natl Acad Sci U S A. 1988; 85:7831–5. [PubMed: 3186693]
81. Baran-Gale J, Fannin EE, Kurtz CL, Sethupathy P. Beta cell 5′-shifted isomiRs are candidate regulatory hubs in type 2 diabetes. PLoS ONE. 2013; 8:e73240. [PubMed: 24039891]
82. Li C, Hung Wong W. Model-based analysis of oligonucleotide arrays: model validation, design issues and standard error application. Genome Biol. 2001; 2:RESEARCH0032. [PubMed: 11532216]
83. Pullen TJ, da Silva Xavier G, Kelsey G, Rutter GA. miR-29a and miR-29b contribute to pancreatic beta-cell-specific silencing of monocarboxylate transporter 1 (Mct1). Mol Cell Biol. 2011; 31:3182–94. [PubMed: 21646425]
84. Zhang Y, Wu L, Wang Y, Zhang M, Li L, Zhu D, Li X, Gu H, Zhang CY, Zen K. Protective role of estrogen-induced miRNA-29 expression in carbon tetrachloride-induced mouse liver injury. J Biol Chem. 2012; 287:14851–62. [PubMed: 22393047]
85. Steneberg P, Sykaras AG, Backlund F, Straseviciene J, Soderstrom I, Edlund H. Hyperinsulinemia enhances hepatic expression of the fatty acid transporter Cd36 and provokes hepatosteatosis and hepatic insulin resistance. J Biol Chem. 2015; 290:19034–43. Epub 2015 Jun 17. 10.1074/jbc.M115.640292 [PubMed: 26085100]
86. Armoni M, Harel C, Karnieli E. Transcriptional regulation of the GLUT4 gene: from PPAR-gamma and FOXO1 to FFA and inflammation. Trends Endocrinol Metab. 2007; 18:100–7. [PubMed: 17317207]
87. Humbert M, Sitbon O, Yaici A, Montani D, O'Callaghan DS, Jais X, Parent F, Savale L, Natali D, Gunther S, Chaouat A, Chabot F, Cordier JF, Habib G, Gressin V, Jing ZC, Souza R, Simonneau G. Survival in incident and prevalent cohorts of patients with pulmonary arterial hypertension. Eur Respir J. 2010; 36:549–55. [PubMed: 20562126]
88. Benza RL, Miller DP, Gomberg-Maitland M, Frantz RP, Foreman AJ, Coffey CS, Frost A, Barst RJ, Badesch DB, Elliott CG, Liou TG, McGoon MD. Predicting survival in pulmonary arterial hypertension: insights from the Registry to Evaluate Early and Long-Term Pulmonary Arterial Hypertension Disease Management (REVEAL). Circulation. 2010; 122:164–72. [PubMed: 20585012]

Clinical Perspectives

Pulmonary arterial hypertension (PAH) is a highly fatal disease of the pulmonary vasculature, with multiple risk factors including the presence of mutations in the bone morphogenetic protein receptor type II (BMPR2) gene, female sex, and abnormal sex hormone levels. Estrogens, such as the metabolite 16α-hydroxyestrone (16αOHE), may contribute to PAH pathogenesis via several mechanisms including alterations in cellular energy metabolism although the precise mechanisms remain unclear. In this study, we demonstrate that increased expression of the miR-29 family is a modifiable feature of BMPR2-associated heritable PAH (HPAH), which may have implications for pathogenesis and treatment including a novel link with 16αOHE. First, we identified increased miR-29 in the lung tissue of human and murine-modeled HPAH. 16αOHE amplified murine-modeled HPAH in association with increased miR-29 levels and molecular markers of insulin resistance. Subsequently, in the setting of 16αOHE exposure, miR-29 antagonism (αmiR29) reduced disease penetrance, hemodynamics, and pulmonary histopathology in murine-modeled HPAH. Furthermore, while correcting the pulmonary hypertension phenotype, treatment with αmiR29 also improved indices of insulin resistance and other markers of abnormal cellular energy metabolism. Together with the observation that female sex and female sex hormones associate with HPAH, our findings support the concept that 16αOHE contributes to HPAH pathogenesis in the setting of a BMPR2 mutation, and this may occur via miR-29 promoting defects in cellular energy metabolism. While further studies are needed, these findings may support novel therapeutic approaches to treat PAH without the complication of direct sex hormone modification.

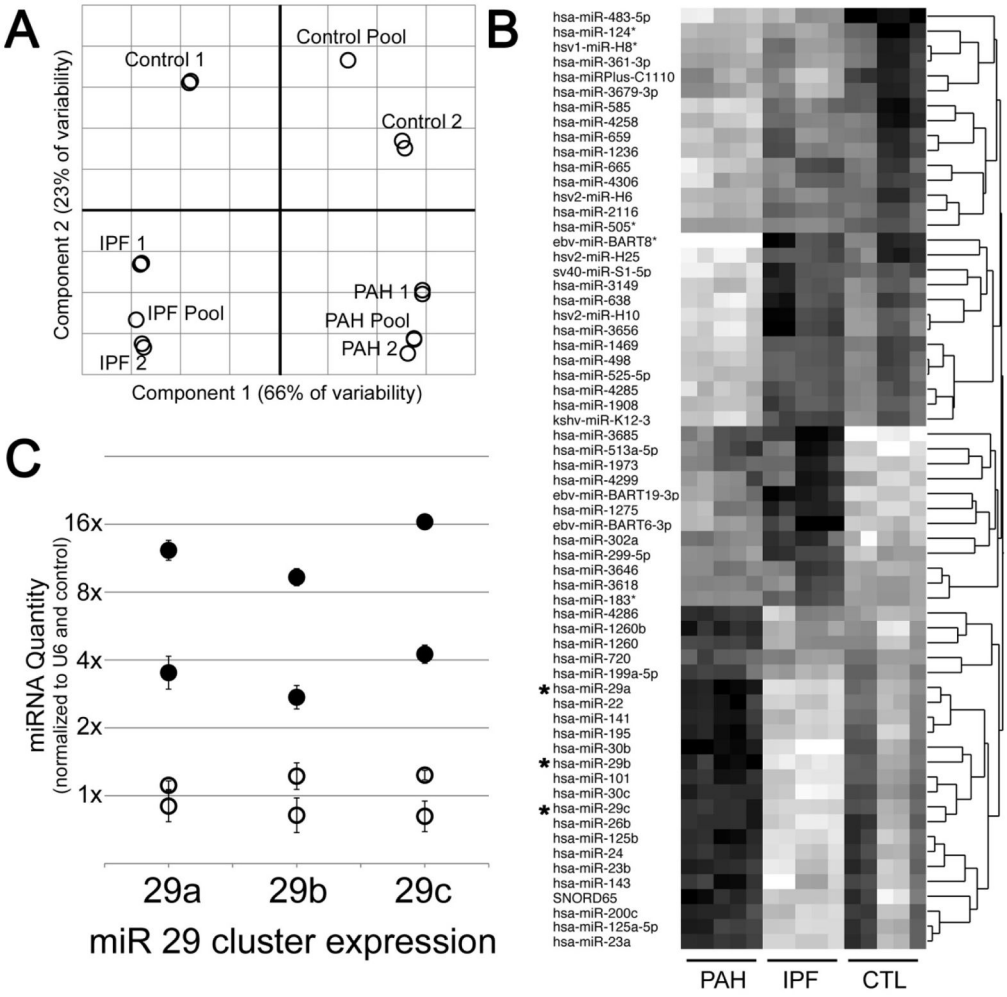

Figure 1.

miRNA arrays show disease-specific effects in human patients (HPAH, n=2; IPF, n=2; Control, n=2). **(A)** Principal Components Analysis shows strong separation between disease states. Each circle represents a sample, with two samples drawn from each of two patients in each disease state. (**B**) Heatmap of 65 miR probe sets differentially regulated in PAH compared to controls, darker color indicates higher expression. miR with an (*) next to them have been described as regulating metabolism. (**C**) Quantitative RT-PCR confirmed upregulation of miR29 family. Open circles are control lung samples; filled circles are PAH patient lung samples. Error bars are SEM. Data were normalized to RNU6B expression and then average of controls set to 1.

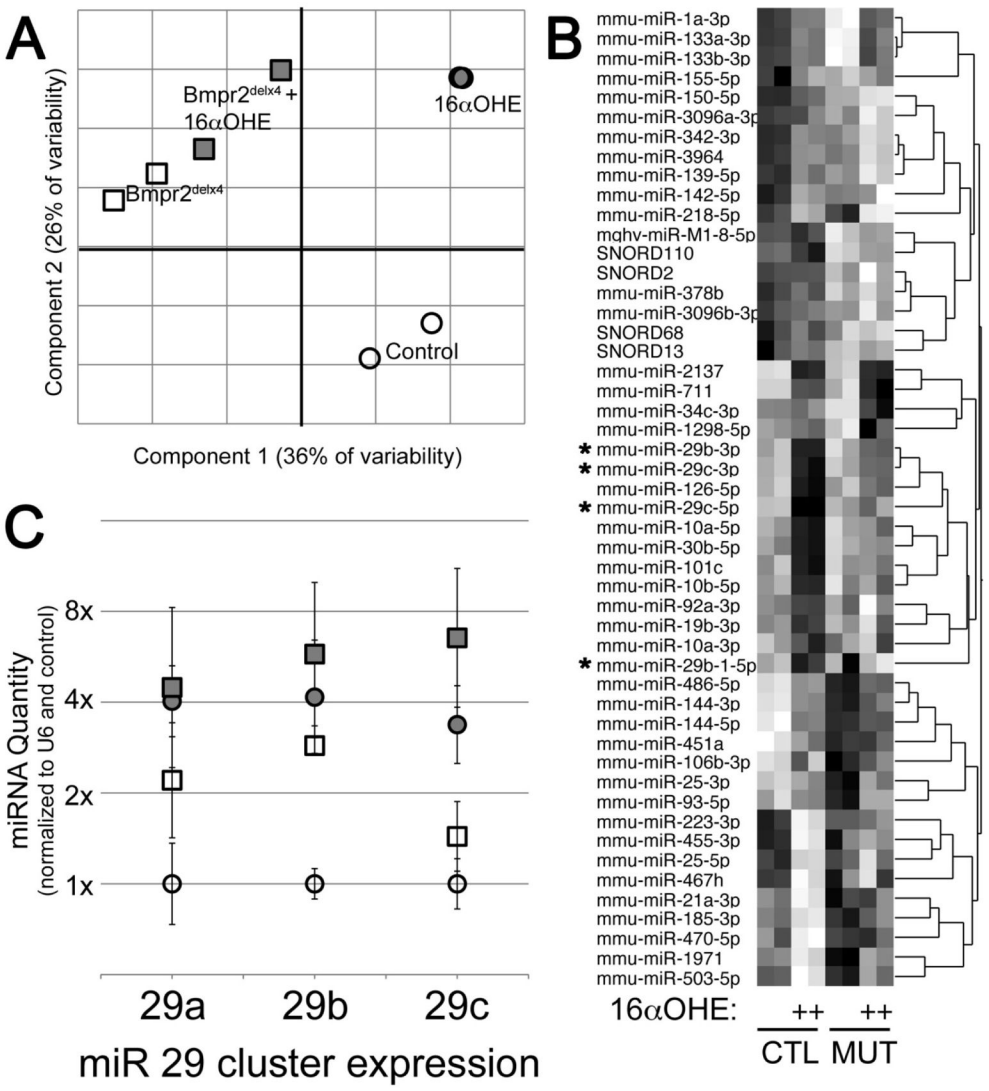

Figure 2.

Male Rosa26-Bmpr2^{delx4+} transgenic mice replicate the miR29 cluster upregulation seen in human patients: mice that received vehicle (n=3) compared to those receiving the estrogen metabolite 16αOHE (n=3): (**A**) Principal Components Analysis shows strong separation between groups, with Bmpr2 mutation causing changes in the component 1 (horizontal) axis, and 16αOHE causing changes in the component 2 (vertical) axis. Each symbol corresponds to a miR array performed on a pool of whole homogenized lung from 3 mice. (**B**) Heatmap of 50 miR probe sets differentially regulated by Bmpr2 mutation or 16αOHE compared to controls, darker color indicates higher expression. miR 29 family are marked with an (*). (**C**) Quantitative RT-PCR confirmed upregulation of miR29 family. Circles are control mouse lung samples; squares are Bmpr2^{delx4+} mutant; filled symbols have been treated with 16αOHE. Error bars are standard deviation. Data were normalized to RNU6B expression and then average of controls set to 1.

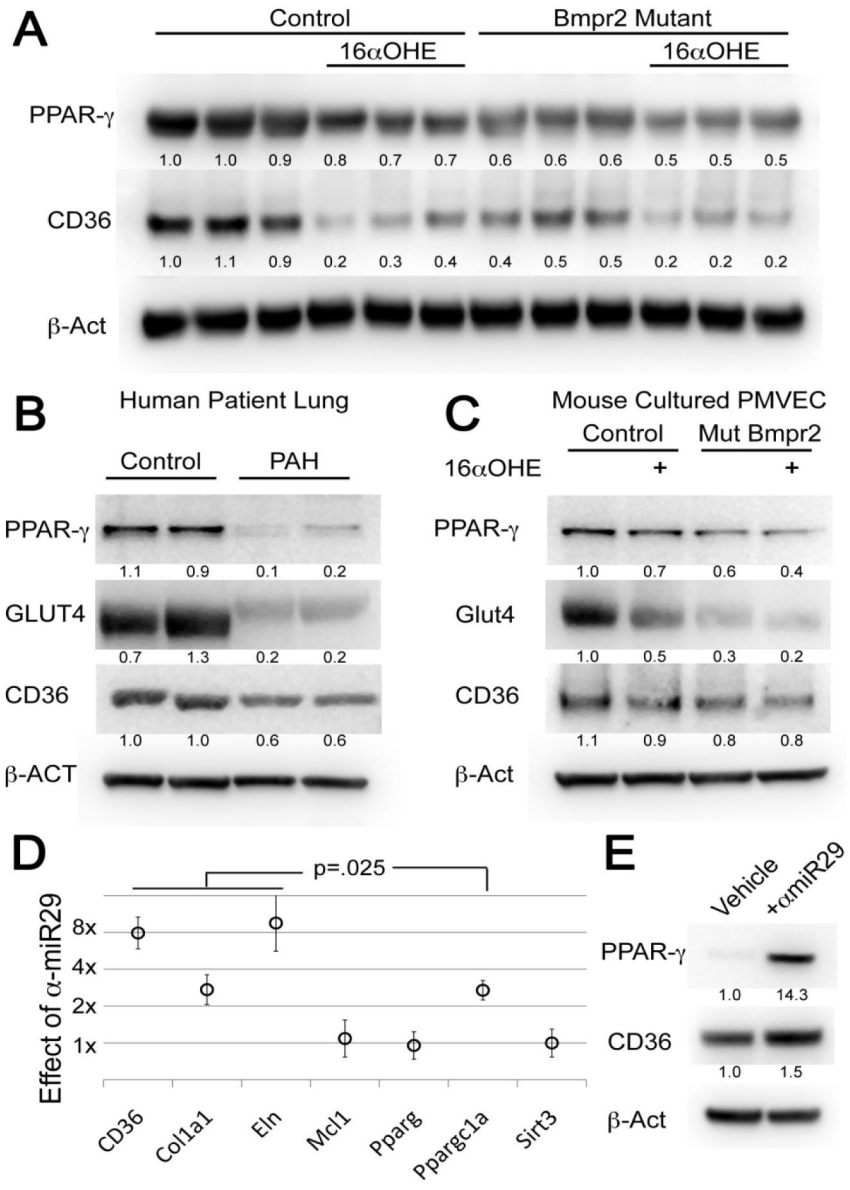

Figure 3.

Molecular markers of insulin resistance are regulated by disease, mutation, and estrogen. (**A**) PPARγ and CD36 are suppressed by both Bmpr2 mutation and 16αOHE treatment in whole mouse lung from male Rosa26-control (n=6) and Rosa26-Bmpr2^{delx4+} mice (n=6). Each column corresponds to a mouse lung. Numbers are densitometry normalized to β-Act. Group differences are significant by two-way ANOVA for PPARγ (mutation effect p<.0001, estrogen effect p=.001, interaction p=.025) and CD36 (mutation effect p=.0003, estrogen effect p<.0001, interaction p=.002) (**B**) PPARγ, GLUT4, and CD36 protein levels are strongly reduced in HPAH patient (n=2) as compared to control (n=2) lung (each lane is a separate individual). **(C)** In cultured murine PMVEC from Rosa26-control (n=2) and Rosa26-Bmpr2^{delx4+} mice (n=2), PPARγ, Glut4, and CD36 protein levels are reduced by Bmpr2 mutation, and reduced further by addition of 16αOHE. **(D)** Transfection of murine

smooth muscle cells with a LNA-modified antisense miRNA-29 causes induction of known targets CD36, Col1a1, Eln, and Ppargc1a (Peroxisome Proliferator-Activated Receptor Gamma, Coactivator 1α), but not related genes, showing specificity. Targets marked are significantly different than vehicle at p=.025 by non-parametric median test.*=**(E)** PPARγ protein is induced 14x and CD36 1.5x by α-miR29 in murine SMC culture.

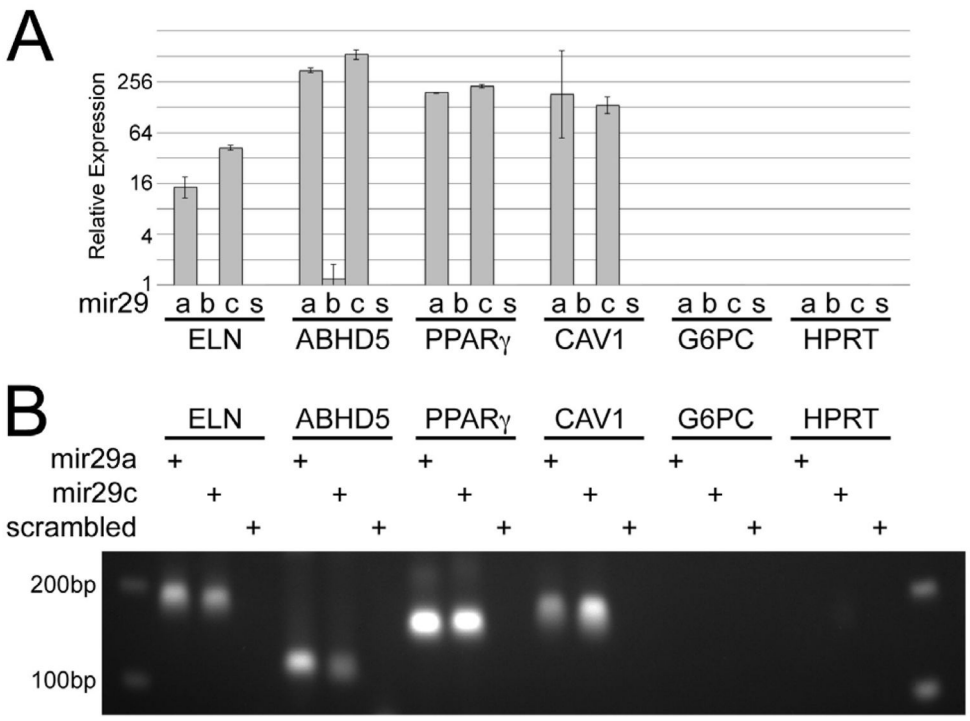

Figure 4.

PPARγ and CAV1, but not CD36, are direct targets of miR-29a and miR-29c. **(A)** miRNA pull-down assays with subsequent quantitative RT-PCR analysis of the affinity purified mRNA demonstrates that the genes PPARγ and CAV1 both are bound at the 3′UTR by miR-29a and miR29c, but not miR29b. Positive and negative controls were included in the assay: as expected, the genes Elastin (ELN) and ABHD5 also are bound (positive controls), while G6PC and HPRT are not (negative controls). **(B)** 1.5% agarose gel loaded with 10μl real-time PCR product, demonstrating gene expression as a function of exposure to miR-29a, miR-29c, or scrambled miRNA duplex. miR-29 family direct targets show clear bands of correct size. Non-target genes show no bands or smear.

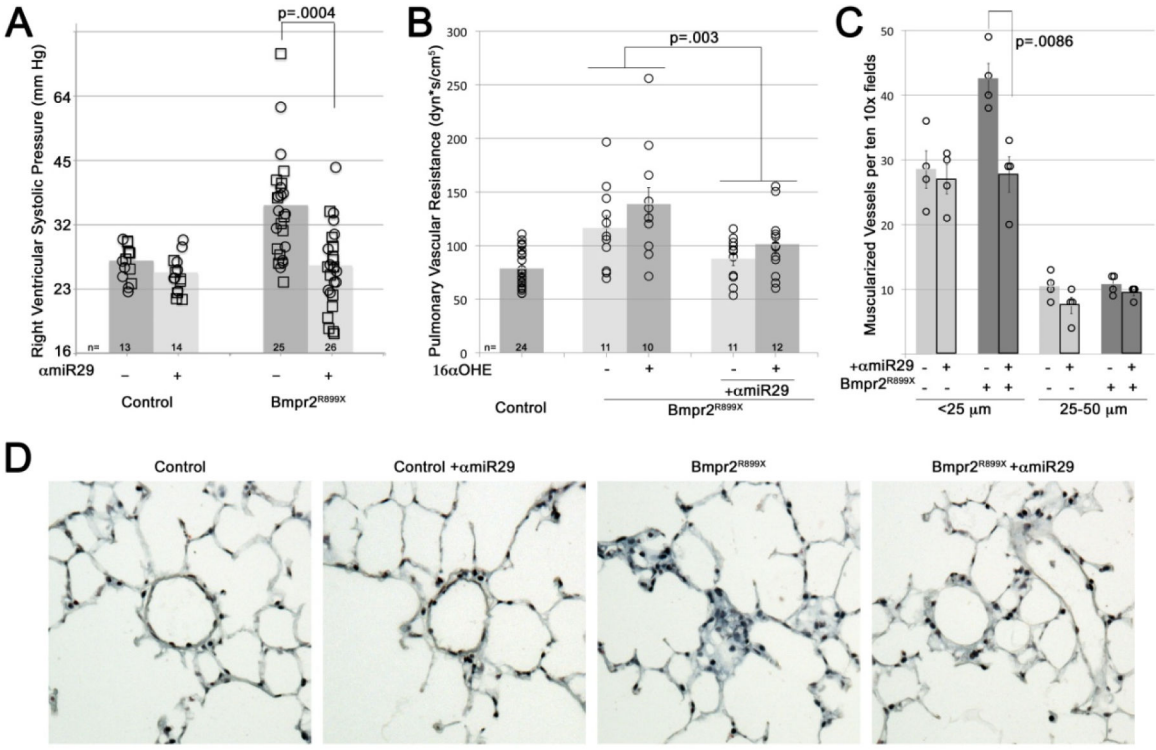

Figure 5.

Antagonism of mir29 significantly improves murine model hemodynamics. **(A)** Weekly injections of anti-miR29 (α-miR-29) for 6 weeks significantly prevents the elevation in RVSP seen with Bmpr2^{R899X} mutation, reducing number of mice with RVSP outside the normal range from 17/25 to 6/26. Each symbol is the RVSP measured from one mouse; bars are averaged log-transformed values. By multiple factor ANOVA, mutation effect was significant at p=.0012, miR effect was significant at p=.0004, and interaction between mutation and miR was significant at p=.0146. All mice were fed western diet. Mice received 16αOHE (squares) or vehicle (circles) in pumps; effect on RVSP was not significant (p=0.41) (Control, n=27; Bmpr2^{R899X}, n=51). Both male and female mice were used; this also had no effect on RVSP (p=0.40). **(B)** Pulmonary vascular resistance: each symbol is the value from one mouse. There was no difference between treatments in control mice; they are combined (n=24; 13 female, 11 male) for clarity. Bmpr2^{R899X} mice were given vehicle and no α-miR29 (n=11; 5 female, 6 male), 16αOHE without α-miR29 (n=11; 7 female, 4 male), vehicle and no α-miR29 (n=11; 6 female, 5 male), or 16αOHE + α-miR29 (n=12; 6 female, 6 male). By multiple factor ANOVA, mutation effect was significant at p=.0005, miR effect in the context of mutation was significant at p=.003, and 16αOHE effect was significant at p=.036. **(C)** α-miR29 treatment reversed increased muscularization seen in Bmpr2^{R899X} mice, as assessed by counting muscularized vessels in ten 10x fields per animal, in four animals per group (each symbol is an animal; each column represents n=4 per group, with 2 female and 2 male per group). By multiple factor ANOVA, mutation was significant at p=.0148, miR effect was significant at p=.0086, and differential miR effect in the context of mutation was significant at p=.0252 (i.e., α-miR29 only reduces muscularization in

Bmpr2^{R899X} mice). **(D)** Examples of fields from trichrome-stained lung sections from control and Bmpr2R899X mice with and without α-miR29 treatment (200X magnification).

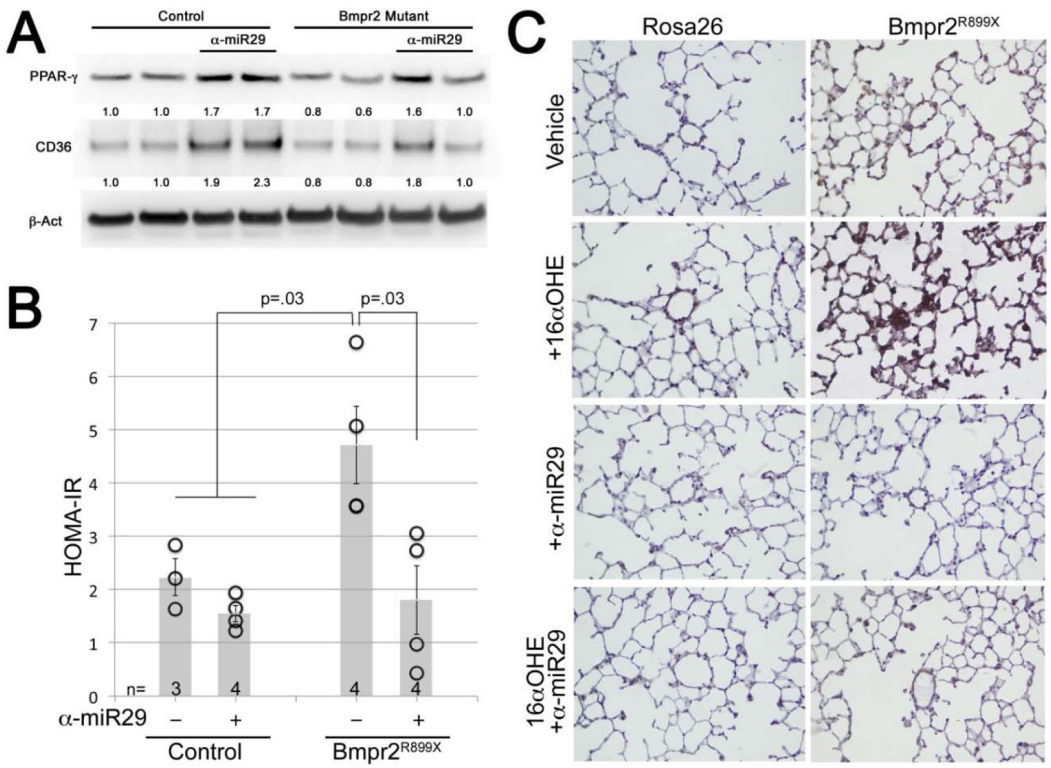

Figure 6.

Treatment with α-miR29 improves metrics of insulin resistance and metabolic dysregulation. **(A)** Weekly injections of α-miR29 for 6 weeks cause significant induction of PPARγ and CD36 protein levels in whole mouse lung, rescuing reduced levels in Bmpr2 mutant. Each lane corresponds to protein from one mouse; numbers are densitometry normalized to βAct. **(B)** α-miR29 treatment prevents elevation of HOMA-IR seen in vehicle treated Bmpr2 mutant mice. Each circle corresponds to one animal measured; error bars are SEM. P values are by non-parametric rank sum test. **(C)** α-miR29 treatment prevents ceramide accumulation in the pulmonary vasculature.

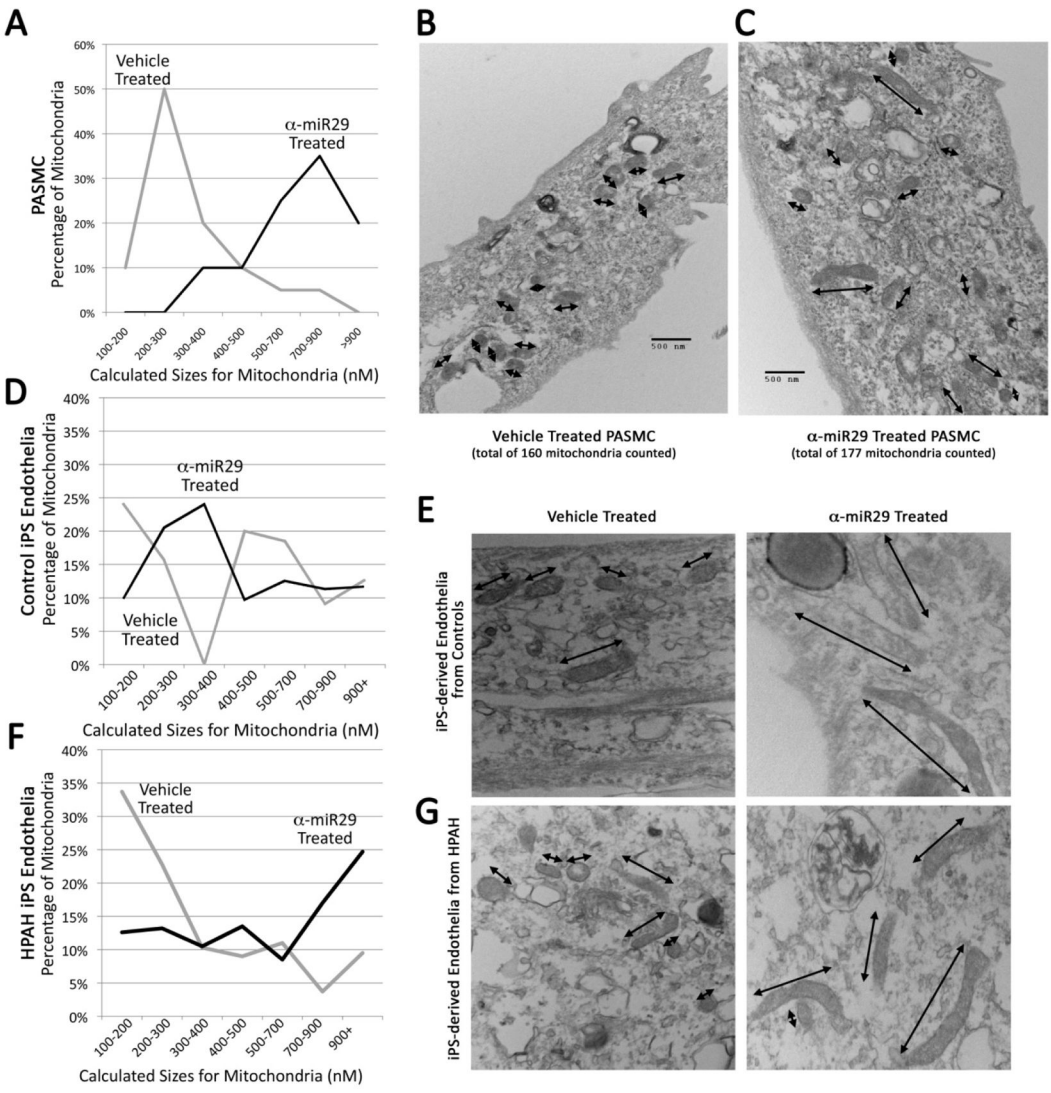

Figure 7.

α-miR29 treatment increases average mitochondrial size. **(A)** A distribution of actual mitochondrial sizes in vehicle or α-miR29 treated cells which is the best fit for the data (Supplement Figure 3) suggests the modal size of α-miR29 treated animals are three times the modal size of vehicle treated. **(B and C)** Examples of PASMCs with vehicle- or α-miR29- treatment, with mitochondrial long axes marked by arrows. **(D)** Mitochondrial sizes in endothelial-like cells differentiated from iPS cells derived from human healthy controls. α-miR29 treatment increases size, but the effect is not strong. **(F)** Mitochondrial sizes in endothelial-like cells differentiated from iPS derived from a BMPR2 mutant PAH patient. α-miR29 treatment causes a near tripling in the average size of mitochondria. **(E)** Example of iPS-derived endothelial-like cells cultured from Control subject in Figure D. (**F**) Example of iPS-derived endothelial-like cells cultured derived from the BMPR2 mutant HPAH patient. Note in Figures E and F that that mitochondrial size is smaller in HPAH, but increases with α-miR29 treatment.

Table 1

Clinical characteristics relevant to PAH diagnosis for human subjects.

PAH-related Phenotypic Data	HPAH 1	HPAH 2	IPF 1	IPF 2	CTL 1	CTL 2
PAH Diagnosis age, yrs	20	13	N/A	N/A	N/A	N/A
Current age yrs	24	13	28	47	23	23
Sex	F	F	F	F	F	F
NYHA functional class, at diagnosis	3	3	N/A	N/A	N/A	N/A
Baseline hemodynamic data, at Dx						
Right atrial pressure mmHg	7	N/A	N/A	N/A	N/A	N/A
Mean pulmonary artery pressure mmHg	66					
Cardiac index $L \cdot min \cdot m^{-2}$	2.5					
Indexed PVR $U \cdot m^2$	12.5					
Responsive to acute vasodilator testing	No					
PAH-specific therapies			N/A	N/A	N/A	N/A
Prostanoids	Yes	No				
Phosphodiesterase-5 inhibitors	No	No				
Endothelin receptor antagonists	No	No				

Note: PAH patient 2 (PAH 2) died of cardiopulmonary arrest prior to cardiac cath. PAH diagnosis made by clinical and echocardiographic data, and autopsy evaluation.

HPAH = heritable pulmonary arterial hypertension

IPF = idiopathic pulmonary fibrosis

PVR = pulmonary vascular resistance

CTL = control